

Chapter 1

MULTIPARTITE ENTANGLEMENT

Peter van Loock

Zentrum für Moderne Optik, Universität Erlangen-Nürnberg, 91058 Erlangen, Germany
vanloock@kerr.physik.uni-erlangen.de

Samuel L. Braunstein

Informatics, Bangor University, Bangor LL57 1UT, United Kingdom
schmuel@sees.bangor.ac.uk

Abstract First, we show how the quantum circuits for generating and measuring multi-party entanglement of qubits can be translated to continuous quantum variables. We derive sufficient inseparability criteria for N -party continuous-variable states and discuss their applicability. Then, we consider a family of multipartite entangled states (multi-party multi-mode states with one mode per party) described by continuous quantum variables and analyze their properties. These states can be efficiently generated using squeezed light and linear optics.

Keywords: Multipartite entanglement, squeezed light

1. INTRODUCTION

What is the main motivation to deal with continuous variables for quantum communication purposes? Quantum communication schemes rely on state preparation, local unitary transformations, measurements, and classical communication. In addition, sometimes shared entanglement is part of the protocol. Within the framework of quantum optics, these ingredients can be efficiently implemented when they are applied to the continuous quadrature amplitudes of electromagnetic modes. For example, the tools for measuring a quadrature with near-unit efficiency or for displacing an optical mode in phase space are provided by homodyne detection and feed-forward techniques, respectively. Continuous-variable entanglement can be efficiently produced using squeezed light and linear optics. In this chapter, we consider a rather general manifes-

tation of continuous-variable entanglement, namely that between an arbitrary number of parties (modes). We will see that even those N -party entangled states where none of the N parties can be separated from the others in the total state vector are comparatively “cheap” in terms of the resources needed: their generation only requires one single-mode squeezed state and $N - 1$ beam splitters.

2. MULTIPARTITE ENTANGLEMENT

The main subject of this section is multi-party entanglement of infinite-dimensional states described by continuous variables. After a few general remarks on entanglement between two and more parties in arbitrary dimensions, we will show how the quantum circuits for creating and measuring qubit entanglement may be translated to continuous variables. Then we derive inequalities that may serve as sufficient multi-party inseparability criteria for continuous-variable states. These are applicable both for a theoretical test and for an indirect experimental verification of multi-party entanglement. Finally, we focus on a family of genuinely multi-party entangled continuous-variable states whose members are fully inseparable with respect to all their parties.

2.1 TWO PARTIES VERSUS MANY PARTIES

Bipartite entanglement, the entanglement of a pair of systems shared by two parties, is easy to handle for **pure states**. For any pure two-party state, orthonormal bases of each subsystem exist, $\{|u_n\rangle\}$ and $\{|v_n\rangle\}$, so that the total state vector can be written in the “Schmidt decomposition” [1] as

$$|\psi\rangle = \sum_n c_n |u_n\rangle |v_n\rangle, \quad (1.1)$$

where the summation goes over the smaller of the dimensionalities of the two subsystems. The Schmidt coefficients c_n are real and non-negative, and satisfy $\sum_n c_n^2 = 1$. The Schmidt decomposition may be obtained by transforming the expansion of an arbitrary pure bipartite state as

$$|\psi\rangle = \sum_{mk} a_{mk} |m\rangle |k\rangle = \sum_{nmk} u_{mn} c_{nn} v_{kn} |m\rangle |k\rangle = \sum_n c_n |u_n\rangle |v_n\rangle, \quad (1.2)$$

with $c_{nn} \equiv c_n$. In the first step, the matrix a with complex elements a_{mk} is diagonalised, $a = ucv^T$, where u and v are unitary matrices and c is a diagonal matrix with non-negative elements. In the second step, we defined $|u_n\rangle \equiv \sum_m u_{mn} |m\rangle$ and $|v_n\rangle \equiv \sum_k v_{kn} |k\rangle$ which form orthonormal sets due to the unitarity of u and v and the orthonormality of $|m\rangle$ and $|k\rangle$. A pure state of two d -level systems (“qudits”) is now maximally entangled when the Schmidt coefficients of its total state vector are all equal. Since the eigenvalues of the

reduced density operator upon tracing out one half of a bipartite state are the Schmidt coefficients squared,

$$\hat{\rho}_1 = \text{Tr}_2 \hat{\rho}_{12} = \text{Tr}_2 |\psi\rangle_{12} \langle \psi| = \sum_n c_n^2 |u_n\rangle_1 \langle u_n|, \quad (1.3)$$

tracing out either qudit of a maximally entangled state leaves the other half in the maximally mixed state $\mathbb{1}/d$. A pure two-party state is factorizable (not entangled) if and only if the number of nonzero Schmidt coefficients is one. Any Schmidt number greater than one indicates entanglement. Thus, the ‘‘majority’’ of pure state vectors in the Hilbert space of two parties are nonmaximally entangled. Furthermore, any pure two-party state is entangled if and only if for suitably chosen observables, it yields a violation of inequalities imposed by local realistic theories [2]. A unique measure of bipartite entanglement for pure states is given by the partial von Neumann entropy, the von Neumann entropy ($-\text{Tr} \hat{\rho} \log \hat{\rho}$) of the remaining system after tracing out either subsystem [3]: $E_{\text{v.N.}} = -\text{Tr} \hat{\rho}_1 \log_d \hat{\rho}_1 = -\sum_n c_n^2 \log_d c_n^2$, ranging between zero and one (in units of ‘‘edits’’).

Mixed states are more subtle, even for only two parties. As for the quantification of bipartite mixed-state entanglement, there are various measures available such as the entanglement of formation and distillation [4]. Only for pure states, these measures coincide and equal the partial von Neumann entropy. The definition of pure-state entanglement via the non-factorizability of the total state vector is generalized to mixed states through non-separability (or inseparability) of the total density operator. A general quantum state of a two-party system is separable if its total density operator is a mixture (a convex sum) of product states [5],

$$\hat{\rho}_{12} = \sum_i P_i \hat{\rho}_{i1} \otimes \hat{\rho}_{i2}. \quad (1.4)$$

Otherwise, it is inseparable¹. In general, it is a non-trivial question whether a given density operator is separable or inseparable. Nonetheless, a very convenient method to test for inseparability is Peres’ partial transpose criterion [6]. For a separable state as in Eq. (1.4), transposition of either density matrix

¹Separable states also exhibit correlations, but those are purely classical. For instance, compare the separable state $\hat{\rho} = \frac{1}{2}(|0\rangle\langle 0| \otimes |0\rangle\langle 0| + |1\rangle\langle 1| \otimes |1\rangle\langle 1|)$ to the pure maximally entangled ‘‘Bell state’’ $|\Phi^+\rangle = \frac{1}{\sqrt{2}}(|0\rangle \otimes |0\rangle + |1\rangle \otimes |1\rangle) = \frac{1}{\sqrt{2}}(|+\rangle \otimes |+\rangle + |-\rangle \otimes |-\rangle)$ with the conjugate basis states $|\pm\rangle = \frac{1}{\sqrt{2}}(|0\rangle \pm |1\rangle)$. The separable state $\hat{\rho}$ is classically correlated only with respect to the predetermined basis $\{|0\rangle, |1\rangle\}$. However, the Bell state $|\Phi^+\rangle$ is a priori quantum correlated in both bases $\{|0\rangle, |1\rangle\}$ and $\{|+\rangle, |-\rangle\}$, and may become a posteriori classically correlated depending on the particular basis choice in a local measurement. Similarly, we will see later that the inseparability criteria for continuous variables need to be expressed in terms of the positions and their conjugate momenta.

yields again a legitimate non-negative density operator with unit trace,

$$\hat{\rho}'_{12} = \sum_i P_i (\hat{\rho}_{i1})^T \otimes \hat{\rho}_{i2}, \quad (1.5)$$

since $(\hat{\rho}_{i1})^T = (\hat{\rho}_{i1})^*$ corresponds to a legitimate density matrix. This is a necessary condition for a separable state, and hence a single negative eigenvalue of the partially transposed density matrix is a sufficient condition for inseparability. In the (2×2) - and (2×3) -dimensional cases (and, for example, for two-mode Gaussian states, see below), this condition is both necessary and sufficient. For any other dimension, negative partial transpose is only sufficient for inseparability [7]². Other sufficient inseparability criteria include violations of inequalities imposed by local realistic theories (though mixed inseparable states do not necessarily lead to such violations), an entropic inequality [namely $E_{\text{v.N.}}(\hat{\rho}_1) > E_{\text{v.N.}}(\hat{\rho}_{12})$, again with $\hat{\rho}_1 = \text{Tr}_2 \hat{\rho}_{12}$] [11], and a condition based on the theory of majorization [12]. Concluding the discussion of two-party entanglement, we emphasize that both the pure-state Schmidt decomposition and the partial transpose criterion for mixed states are also applicable to infinite dimensions. An example for the infinite-dimensional Schmidt decomposition is the two-mode squeezed vacuum state in the Fock (photon number) basis [13]. The unphysical operation (a positive, but not completely positive map) that corresponds to the transposition is time reversal [14]: in terms of continuous variables, any separable two-party state remains a legitimate state after the transformation $(x_1, p_1, x_2, p_2) \rightarrow (x_1, -p_1, x_2, p_2)$, where (x_i, p_i) are the phase-space variables (positions and momenta) for example in the Wigner representation. However, arbitrary inseparable states may be turned into unphysical states, and furthermore, inseparable two-party two-mode Gaussian states always become unphysical via this transformation [14].

Multipartite entanglement, the entanglement shared by more than two parties, is a more complex issue. For **pure** multi-party states, a Schmidt decomposition does not exist in general. The total state vector then cannot be written as a single sum over orthonormal basis states. There is, however, one very important representative of multipartite entanglement which does have the form of a multi-party Schmidt decomposition, namely the Greenberger-Horne-

²Inseparable states with positive partial transpose cannot be distilled to a maximally entangled state via local operations and classical communication. They are so-called “bound entangled” [8]. The converse, however, does not hold. An explicit example of a bound entangled state with negative partial transpose was given in Ref. [9]. In other words, not all entangled states that reveal their inseparability through negative partial transpose are distillable or “free entangled”. On the other hand, any state $\hat{\rho}_{12}$ that violates the so-called reduction criterion, $\hat{\rho}_1 \otimes \mathbf{1} - \hat{\rho}_{12} \geq 0$ or $\mathbf{1} \otimes \hat{\rho}_2 - \hat{\rho}_{12} \geq 0$, is both inseparable and distillable [10]. This reduction criterion is in general weaker than the partial transpose criterion and the two criteria are equivalent in the (2×2) - and (2×3) -dimensional cases.

Zeilinger (GHZ) state [15]

$$|\text{GHZ}\rangle = \frac{1}{\sqrt{2}} (|000\rangle + |111\rangle) , \quad (1.6)$$

here given as a three-qubit state. Although there is no rigorous definition of maximally entangled multi-party states due to the lack of a general Schmidt decomposition, the form of the GHZ state with all ‘‘Schmidt coefficients’’ equal suggests that it exhibits maximum multipartite entanglement. In fact, there are various reasons for assigning the attribute ‘‘maximally entangled’’ to the N -party GHZ states $[(|000 \cdots 000\rangle + |111 \cdots 111\rangle)/\sqrt{2}]$. For example, they yield the maximum violations of multi-party inequalities imposed by local realistic theories [16]. Further, their entanglement heavily relies on all parties, and if examined pairwise they do not contain simple bipartite entanglement (see below).

For the case of three qubits, any pure and fully entangled state can be transformed to either the GHZ state or the so-called W state [17],

$$|\text{W}\rangle = \frac{1}{\sqrt{3}} (|100\rangle + |010\rangle + |001\rangle) , \quad (1.7)$$

via stochastic local operations and classical communication (‘‘SLOCC’’, where stochastic means that the state is transformed with non-zero probability). Thus, with respect to SLOCC, there are two inequivalent classes of genuine tripartite entanglement, represented by the GHZ and the W state. Genuinely or fully tripartite entangled here means that the entanglement of the three-qubit state is not just present between two parties while the remaining party can be separated by a tensor product. Though genuinely tripartite, the entanglement of the W state is also ‘‘readily bipartite’’. This means that the remaining two-party state after tracing out one party,

$$\text{Tr}_1 |\text{W}\rangle\langle\text{W}| = \frac{1}{3} (|00\rangle\langle 00| + |10\rangle\langle 10| + |01\rangle\langle 01| + |01\rangle\langle 10| + |10\rangle\langle 01|) , \quad (1.8)$$

is inseparable which can be verified by taking the partial transpose [the eigenvalues are $1/3, 1/3, (1 \pm \sqrt{5})/6$]. This is in contrast to the GHZ state where tracing out one party yields the separable two-qubit state

$$\begin{aligned} \text{Tr}_1 |\text{GHZ}\rangle\langle\text{GHZ}| &= \frac{1}{2} (|00\rangle\langle 00| + |11\rangle\langle 11|) \\ &= \frac{1}{2} (|0\rangle\langle 0| \otimes |0\rangle\langle 0| + |1\rangle\langle 1| \otimes |1\rangle\langle 1|) . \end{aligned} \quad (1.9)$$

Note that this is not the maximally mixed state of two qubits, $\mathbb{1}^{\otimes 2}/4$. The maximally mixed state of one qubit, however, is obtained after tracing out two

parties of the GHZ state. Maximum bipartite entanglement is available from the GHZ state through a local measurement of one party in the conjugate basis $\{(|0\rangle \pm |1\rangle)/\sqrt{2}\}$ (plus classical communication about the result),

$$\frac{\frac{1}{2}(|0\rangle_1 \pm |1\rangle_1) \langle 1| \langle 0| \pm \langle 1| \langle 1| | \text{GHZ} \rangle}{\|\frac{1}{2}(|0\rangle_1 \pm |1\rangle_1) \langle 1| \langle 0| \pm \langle 1| \langle 1| | \text{GHZ} \rangle\|} = \frac{1}{\sqrt{2}}(|0\rangle_1 \pm |1\rangle_1) \otimes |\Phi^\pm\rangle. \quad (1.10)$$

Here, $|\Phi^\pm\rangle$ are two of the four Bell states, $|\Phi^\pm\rangle = (|00\rangle \pm |11\rangle)/\sqrt{2}$, $|\Psi^\pm\rangle = (|01\rangle \pm |10\rangle)/\sqrt{2}$.

What can be said about arbitrary **mixed** entangled states of more than two parties? There is of course an immense variety of inequivalent classes of multi-party mixed states [e.g., five classes of three-qubit states of which the extreme cases are the fully separable ($\hat{\rho} = \sum_i P_i \hat{\rho}_{i1} \otimes \hat{\rho}_{i2} \otimes \hat{\rho}_{i3}$) and the fully (genuinely) inseparable states [18]]. In general, multi-party inseparability criteria cannot be formulated in such a compact form as the two-party partial transpose criterion. Similarly, the quantification of multipartite entanglement, even for pure states, is still subject of current research. Existing multi-party entanglement measures do not appear to be unique as is the partial von Neumann entropy for pure two-party states. Furthermore, violations of multi-party inequalities imposed by local realism do not necessarily imply genuine multi-party inseparability. In the case of continuous variables, we may now focus on the following questions: How can we generate, measure, and (theoretically and experimentally) verify genuine multipartite entangled states? How do the continuous-variable states compare to their qubit counterparts with respect to various properties?

2.2 CREATING MULTIPARTITE ENTANGLEMENT

A compact way to describe how entanglement may be created is in terms of a quantum circuit. Quantum circuits consist of a sequence of unitary transformations (quantum gates), sometimes supplemented by measurements. A quantum circuit is independent of a particular physical realization.

Let us consider the generation of entanglement between arbitrarily many qubits. The quantum circuit shall turn N independent qubits into an N -partite entangled state. Initially, the N qubits shall be in the eigenstate $|0\rangle$. All we need is a circuit with the following two elementary gates: the Hadamard gate, acting on a single qubit as

$$|0\rangle \longrightarrow \frac{1}{\sqrt{2}}(|0\rangle + |1\rangle), \quad |1\rangle \longrightarrow \frac{1}{\sqrt{2}}(|0\rangle - |1\rangle), \quad (1.11)$$

and the controlled-NOT (C-NOT) gate, a two-qubit operation acting as

$$|00\rangle \longrightarrow |00\rangle, \quad |01\rangle \longrightarrow |01\rangle, \quad |10\rangle \longrightarrow |11\rangle, \quad |11\rangle \longrightarrow |10\rangle. \quad (1.12)$$

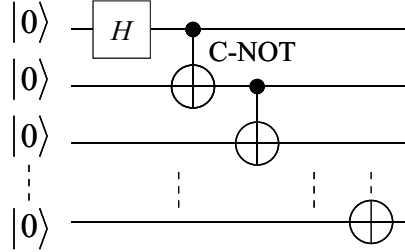


Figure 1.1 Quantum circuit for generating the N -qubit GHZ state. The gates (unitary transformations) are a Hadamard gate (“ H ”) and pairwise acting C-NOT gates.

The first qubit (control qubit) remains unchanged under the C-NOT. The second qubit (target qubit) is flipped if the control qubit is set to 1, and is left unchanged otherwise. Equivalently, we can describe the action of the C-NOT gate by $|y_1, y_2\rangle \rightarrow |y_1, y_1 \oplus y_2\rangle$ with $y_1, y_2 = 0, 1$ and the addition modulo two \oplus . The N -partite entangled output state of the circuit (see Fig. 1.1) is the N -qubit GHZ state.

Let us translate the qubit quantum circuit to continuous variables [19]. The position and momentum variables x and p (units-free with $\hbar = \frac{1}{2}$, $[\hat{x}_l, \hat{p}_k] = i\delta_{lk}/2$) may correspond to the quadrature amplitudes of a single electromagnetic mode, i.e., the real and imaginary part of the single mode’s annihilation operator: $\hat{a} = \hat{x} + i\hat{p}$. At this stage, it is convenient to consider position and momentum eigenstates. We may now replace the Hadamard by a Fourier transform,

$$\mathcal{F}|x\rangle_{\text{position}} = \frac{1}{\sqrt{\pi}} \int_{-\infty}^{\infty} dy e^{2ixy} |y\rangle_{\text{position}} = |p = x\rangle_{\text{momentum}}, \quad (1.13)$$

and the C-NOT gates by appropriate beam splitter operations³. The input states are taken to be zero-position eigenstates $|x = 0\rangle$. The sequence of beam splitter operations $\hat{B}_{jk}(\theta)$ is provided by a network of ideal phase-free beam splitters (with typically asymmetric transmittance and reflectivity) acting on the position eigenstates as

$$\hat{B}_{12}(\theta)|x_1, x_2\rangle = |x_1 \sin \theta + x_2 \cos \theta, x_1 \cos \theta - x_2 \sin \theta\rangle = |x'_1, x'_2\rangle. \quad (1.14)$$

³A possible continuous-variable generalization of the C-NOT gate is $|x_1, x_2\rangle \rightarrow |x_1, x_1 + x_2\rangle$, where the addition modulo two of the qubit C-NOT, $|y_1, y_2\rangle \rightarrow |y_1, y_1 \oplus y_2\rangle$ with $y_1, y_2 = 0, 1$, has been replaced by the normal addition. However, for the quantum circuit here, a beam splitter operation as described by Eq. (1.14) is a suitable substitute for the generalized C-NOT gate.

Now we apply this sequence of beam splitters (making an “ N -splitter”),

$$\hat{B}_{N-1N}(\pi/4)\hat{B}_{N-2N-1}\left(\sin^{-1}1/\sqrt{3}\right)\times\cdots\times\hat{B}_{12}\left(\sin^{-1}1/\sqrt{N}\right), \quad (1.15)$$

to a zero-momentum eigenstate $|p=0\rangle\propto\int dx|x\rangle$ of mode 1 (the Fourier transformed zero-position eigenstate) and $N-1$ zero-position eigenstates $|x=0\rangle$ in modes 2 through N . We obtain the entangled N -mode state $\int dx|x,x,\dots,x\rangle$. This state is an eigenstate with total momentum zero and all relative positions $x_i-x_j=0$ ($i,j=1,2,\dots,N$). It is clearly an analogue to the qubit GHZ state with perfect correlations among the quadratures. However, it is an unphysical and unnormalizable state (e.g., for two modes, it corresponds to the maximally entangled, infinitely squeezed two-mode squeezed vacuum state with infinite energy). Rather than sending infinitely squeezed position eigenstates through the entanglement-generating circuit, we will now use finitely squeezed states.

In the Heisenberg representation, an ideal phase-free beam splitter operation acting on two modes with annihilation operators \hat{c}_k and \hat{c}_l is described by

$$\begin{pmatrix} \hat{c}'_k \\ \hat{c}'_l \end{pmatrix} = \begin{pmatrix} \sin\theta & \cos\theta \\ \cos\theta & -\sin\theta \end{pmatrix} \begin{pmatrix} \hat{c}_k \\ \hat{c}_l \end{pmatrix}. \quad (1.16)$$

Let us now define a matrix $B_{kl}(\theta)$ which is an N -dimensional identity matrix with the entries I_{kk}, I_{kl}, I_{lk} , and I_{ll} replaced by the corresponding entries of the above beam splitter matrix. Thus, the matrix for the N -splitter becomes

$$\begin{aligned} \mathcal{U}(N) \equiv & B_{N-1N}\left(\sin^{-1}\frac{1}{\sqrt{2}}\right)B_{N-2N-1}\left(\sin^{-1}\frac{1}{\sqrt{3}}\right) \\ & \times\cdots\times B_{12}\left(\sin^{-1}\frac{1}{\sqrt{N}}\right). \end{aligned} \quad (1.17)$$

The entanglement-generating circuit is now applied to N position-squeezed vacuum modes. In other words, one momentum-squeezed and $N-1$ position-squeezed vacuum modes are coupled by an N -splitter,

$$\left(\hat{a}'_1\hat{a}'_2\cdots\hat{a}'_N\right)^T = \mathcal{U}(N)\left(\hat{a}_1\hat{a}_2\cdots\hat{a}_N\right)^T, \quad (1.18)$$

where the input modes are squeezed [13] according to

$$\begin{aligned} \hat{a}_1 &= \cosh r_1\hat{a}_1^{(0)} + \sinh r_1\hat{a}_1^{(0)\dagger}, \\ \hat{a}_i &= \cosh r_2\hat{a}_i^{(0)} - \sinh r_2\hat{a}_i^{(0)\dagger}, \end{aligned} \quad (1.19)$$

with $i=2,3,\dots,N$ and vacuum modes labeled by the superscript ‘(0)’. In terms of the input quadratures, we have

$$\begin{aligned} \hat{x}_1 &= e^{+r_1}\hat{x}_1^{(0)}, & \hat{p}_1 &= e^{-r_1}\hat{p}_1^{(0)}, \\ \hat{x}_i &= e^{-r_2}\hat{x}_i^{(0)}, & \hat{p}_i &= e^{+r_2}\hat{p}_i^{(0)}, \end{aligned} \quad (1.20)$$

for $\hat{a}_j = \hat{x}_j + i\hat{p}_j$ ($j = 1, 2, \dots, N$). The squeezing parameters r_1 and r_2 determine the degree of squeezing of the momentum-squeezed and the $N - 1$ position-squeezed modes, respectively. The correlations between the output quadratures are revealed by the arbitrarily small noise in the relative positions and the total momentum for sufficiently large squeezing r_1 and r_2 ,

$$\langle (\hat{x}'_k - \hat{x}'_l)^2 \rangle = e^{-2r_2}/2, \quad \langle (\hat{p}'_1 + \hat{p}'_2 + \dots + \hat{p}'_N)^2 \rangle = Ne^{-2r_1}/4, \quad (1.21)$$

for $k \neq l$ ($k, l = 1, 2, \dots, N$) and $\hat{a}'_k = \hat{x}'_k + i\hat{p}'_k$. Note that all modes involved have zero mean values, thus the variances and the second moments are identical.

2.3 MEASURING MULTIPARTITE ENTANGLEMENT

Rather than constructing a circuit for generating entangled states, now our task shall be the measurement of multi-party entanglement, i.e., the projection onto the basis of maximally entangled multi-party states. For qubits, it is well-known that this can be achieved simply by inverting the above entanglement-generating circuit (a similar strategy also works for d -level systems [20]). The GHZ basis states for N qubits read

$$\begin{aligned} |\Psi_{n,m_1,m_2,\dots,m_{N-1}}\rangle &= \frac{1}{\sqrt{2}} (|0\rangle \otimes |m_1\rangle \otimes |m_2\rangle \otimes \dots \otimes |m_{N-1}\rangle \\ &+ (-1)^n |1\rangle \otimes |1 \oplus m_1\rangle \otimes |1 \oplus m_2\rangle \otimes \dots \otimes |1 \oplus m_{N-1}\rangle), \end{aligned} \quad (1.22)$$

where $n, m_1, m_2, \dots, m_{N-1} = 0, 1$. The projection onto the basis states $\{|\Psi_{n,m_1,m_2,\dots,m_{N-1}}\rangle\}$ is accomplished when the output states of the inverted circuit (see Fig. 1.1),

$$\begin{aligned} &(\text{CNOT}_{N-1N} \text{CNOT}_{N-2N-1} \dots \text{CNOT}_{12} H_1)^{-1} \\ &= H_1 \text{CNOT}_{12} \text{CNOT}_{23} \dots \text{CNOT}_{N-1N}, \end{aligned} \quad (1.23)$$

are measured in the computational basis. Eventually, $\{|\Psi_{n,m_1,m_2,\dots,m_{N-1}}\rangle\}$ are distinguished via the measured output states

$$|n\rangle \otimes |m_1\rangle \otimes |m_1 \oplus m_2\rangle \otimes |m_2 \oplus m_3\rangle \otimes \dots \otimes |m_{N-2} \oplus m_{N-1}\rangle. \quad (1.24)$$

Reentering the domain of continuous variables, let us now introduce the maximally entangled states

$$\begin{aligned} |\Psi(v, u_1, u_2, \dots, u_{N-1})\rangle &= \frac{1}{\sqrt{\pi}} \int_{-\infty}^{\infty} dx e^{2ivx} |x\rangle \otimes |x - u_1\rangle \\ &\otimes |x - u_1 - u_2\rangle \otimes \dots \otimes |x - u_1 - u_2 - \dots - u_{N-1}\rangle. \end{aligned} \quad (1.25)$$

Since $\int_{-\infty}^{\infty} |x\rangle\langle x| = \mathbb{1}$ and $\langle x|x'\rangle = \delta(x - x')$, they form a complete,

$$\begin{aligned} &\int_{-\infty}^{\infty} dv du_1 du_2 \dots du_{N-1} |\Psi(v, u_1, u_2, \dots, u_{N-1})\rangle \langle \Psi(v, u_1, u_2, \dots, u_{N-1})| \\ &= \mathbb{1}^{\otimes N}, \end{aligned} \quad (1.26)$$

and orthogonal,

$$\begin{aligned} & \langle \Psi(v, u_1, u_2, \dots, u_{N-1}) | \Psi(v', u'_1, u'_2, \dots, u'_{N-1}) \rangle \\ & = \delta(v - v') \delta(u_1 - u'_1) \delta(u_2 - u'_2) \cdots \delta(u_{N-1} - u'_{N-1}), \end{aligned} \quad (1.27)$$

set of basis states for N modes. For creating continuous-variable entanglement, we simply replaced the C-NOT gates by appropriate beam splitter operations. Let us employ the same strategy here in order to measure continuous-variable entanglement. In other words, a projection onto the continuous-variable GHZ basis $\{|\Psi(v, u_1, u_2, \dots, u_{N-1})\rangle\}$ shall be performed by applying an inverse N -splitter followed by a Fourier transform of mode 1 and by subsequently measuring the positions of all modes. For an N -mode state with modes $\hat{b}_1, \hat{b}_2, \dots, \hat{b}_N$, this means that we effectively measure $\text{Im } \hat{b}'_1 \equiv \hat{p}'_1, \text{Re } \hat{b}'_2 \equiv \hat{x}'_2, \text{Re } \hat{b}'_3 \equiv \hat{x}'_3, \dots, \text{Re } \hat{b}'_N \equiv \hat{x}'_N$, with

$$\left(\hat{b}'_1 \quad \hat{b}'_2 \quad \cdots \quad \hat{b}'_N \right)^T = \mathcal{U}^\dagger(N) \left(\hat{b}_1 \quad \hat{b}_2 \quad \cdots \quad \hat{b}_N \right)^T. \quad (1.28)$$

For instance, in the three-mode case, the measured observables are

$$\begin{aligned} \hat{p}'_1 &= \frac{1}{\sqrt{3}}(\hat{p}_1 + \hat{p}_2 + \hat{p}_3), \\ \hat{x}'_2 &= \sqrt{\frac{2}{3}}\hat{x}_1 - \frac{1}{\sqrt{6}}(\hat{x}_2 + \hat{x}_3), \\ \hat{x}'_3 &= \frac{1}{\sqrt{2}}(\hat{x}_2 - \hat{x}_3), \end{aligned} \quad (1.29)$$

where here $\hat{b}_j = \hat{x}_j + i\hat{p}_j$. In fact, in a single shot, the quantities $v/\sqrt{3}$, $\sqrt{2/3}(u_1 + u_2/2)$, and $u_2/\sqrt{2}$ are determined through these measurements, and so are all the parameters $v \equiv p_1 + p_2 + p_3$, $u_1 \equiv x_1 - x_2$, and $u_2 \equiv x_2 - x_3$ required to detect the basis state $|\Psi(v, u_1, u_2)\rangle$ from Eq. (1.25) with $N = 3$. In general, for arbitrary N , the measurements yield $p'_1 = v/\sqrt{N}$ and

$$\begin{aligned} x'_2 &= \sqrt{\frac{N-1}{N}} \left(u_1 + \frac{N-2}{N-1} \left(u_2 + \frac{N-3}{N-2} (u_3 + \cdots) \right) \right), \\ &\quad \vdots \qquad \qquad \qquad \vdots \qquad \qquad \qquad \vdots \\ x'_{N-3} &= \sqrt{\frac{4}{5}} \left(u_{N-4} + \frac{3}{4} \left(u_{N-3} + \frac{2}{3} \left(u_{N-2} + \frac{1}{2} u_{N-1} \right) \right) \right), \\ x'_{N-2} &= \sqrt{\frac{3}{4}} \left(u_{N-3} + \frac{2}{3} \left(u_{N-2} + \frac{1}{2} u_{N-1} \right) \right), \\ x'_{N-1} &= \sqrt{\frac{2}{3}} \left(u_{N-2} + \frac{1}{2} u_{N-1} \right), \\ x'_N &= \frac{1}{\sqrt{2}} u_{N-1}, \end{aligned} \quad (1.30)$$

where $v \equiv p_1 + p_2 + \dots + p_N$, $u_1 \equiv x_1 - x_2$, $u_2 \equiv x_2 - x_3, \dots$, and $u_{N-1} \equiv x_{N-1} - x_N$. This confirms that the inverse N -splitter combined with the appropriate homodyne detections (that is tools solely from linear optics) enables in principle a complete distinction of the basis states $\{|\Psi(v, u_1, u_2, \dots, u_{N-1})\rangle\}$ in Eq. (1.25). More precisely, the fidelity of the state discrimination can be arbitrarily high for sufficiently good accuracy of the homodyne detectors. We may conclude that the requirements of such a ‘‘GHZ state analyzer’’ for continuous variables are easily met by current experimental capabilities. This is in contrast to the GHZ state analyzer for photonic qubits [capable of discriminating or measuring states like those in Eq. (1.22)]. Although arbitrarily high fidelity can be approached in principle using linear optics and photon number detectors, one would need sufficiently many, highly entangled auxiliary photons and detectors resolving correspondingly large photon numbers [21, 20]. Neither of these requirements is met by current technology. Of course, the C-NOT gates of a qubit GHZ state measurement device can in principle be implemented via the so-called cross Kerr effect using nonlinear optics. However, on the single-photon level, this would require optical nonlinearities of exotic strength.

In this section, we have shown how measurements onto the maximally entangled continuous-variable GHZ basis can be realized using linear optics and quadrature detections. These schemes are an extension of the well-known two-party case, where the continuous-variable Bell basis [Eq. (1.25) with $N = 2$] is the analogue to the qubit Bell states [Eq. (1.22) with $N = 2$]. The continuous-variable and the qubit Bell states form those measurement bases that were used in the quantum teleportation experiments [22] and [23, 24], respectively. The extension of measurements onto the maximally entangled basis to more than two parties and their potential optical realization in the continuous-variable realm might be relevant to multi-party quantum communication protocols such as the multi-party generalization of entanglement swapping [25]. However, the entanglement resources in a continuous-variable protocol, namely the entangled continuous-variable states that are producible with squeezed light and beam splitters, exhibit only imperfect entanglement due to the finite degree of the squeezing. When can we actually be sure that they are multi-party entangled at all? In the next section, we will address this question and discuss criteria for the theoretical and the experimental verification of multipartite continuous-variable entanglement.

2.4 SUFFICIENT INSEPARABILITY CRITERIA

For continuous-variable two-party states, an inseparability criterion can be derived that does not rely on the partial transpose. It is based on the variances of quadrature combinations such as $\hat{x}_1 - \hat{x}_2$ and $\hat{p}_1 + \hat{p}_2$, motivated by the fact that the maximally entangled bipartite state $\int dx |x, x\rangle$ is a (zero-)eigenstate

of these two combinations [26]. Similarly, in a continuous-variable Bell measurement, the quadrature combinations $\hat{x}_1 - \hat{x}_2$ and $\hat{p}_1 + \hat{p}_2$ are the relevant observables to be detected. Hence, for two modes, applying the variance-based inseparability criterion and measuring in the maximally entangled basis can both be accomplished by equal means, namely a single beam splitter and two homodyne detectors. In other words, the effectively inverse circuit for the generation of bipartite entanglement provides the recipe for both measuring maximum entanglement and verifying nonmaximum entanglement. When looking for multi-party inseparability criteria for arbitrarily many modes, it seems to be natural to pursue a similar strategy. We are therefore aiming at a criterion which is based on the variances of those quadrature combinations that are the measured observables in a continuous-variable GHZ measurement.

Let us consider three modes. According to Eq. (1.29), we define the operators

$$\begin{aligned}\hat{u} &\equiv \frac{1}{\sqrt{2}}(\hat{x}_2 - \hat{x}_3), \\ \hat{v} &\equiv \sqrt{\frac{2}{3}}\hat{x}_1 - \frac{1}{\sqrt{6}}(\hat{x}_2 + \hat{x}_3), \\ \hat{w} &\equiv \frac{1}{\sqrt{3}}(\hat{p}_1 + \hat{p}_2 + \hat{p}_3) \times \sqrt{2},\end{aligned}\tag{1.31}$$

where we added a factor of $\sqrt{2}$ in \hat{w} compared to the first line of Eq. (1.29). Let us further assume that the three-party state $\hat{\rho}$ is fully separable and can be written as a mixture of tripartite product states,

$$\hat{\rho} = \sum_i P_i \hat{\rho}_{i1} \otimes \hat{\rho}_{i2} \otimes \hat{\rho}_{i3}.\tag{1.32}$$

Using this state, we can calculate the total variance of the operators in Eq. (1.31),

$$\begin{aligned}&\langle(\Delta\hat{u})^2\rangle_\rho + \langle(\Delta\hat{v})^2\rangle_\rho + \langle(\Delta\hat{w})^2\rangle_\rho \\ &= \sum_i P_i (\langle\hat{u}^2\rangle_i + \langle\hat{v}^2\rangle_i + \langle\hat{w}^2\rangle_i) - \langle\hat{u}\rangle_\rho^2 - \langle\hat{v}\rangle_\rho^2 - \langle\hat{w}\rangle_\rho^2 \\ &= \sum_i P_i \frac{2}{3} (\langle\hat{x}_1^2\rangle_i + \langle\hat{x}_2^2\rangle_i + \langle\hat{x}_3^2\rangle_i + \langle\hat{p}_1^2\rangle_i + \langle\hat{p}_2^2\rangle_i + \langle\hat{p}_3^2\rangle_i) \\ &\quad - \sum_i P_i \frac{2}{3} (\langle\hat{x}_1\rangle_i\langle\hat{x}_2\rangle_i + \langle\hat{x}_1\rangle_i\langle\hat{x}_3\rangle_i + \langle\hat{x}_2\rangle_i\langle\hat{x}_3\rangle_i \\ &\quad - 2\langle\hat{p}_1\rangle_i\langle\hat{p}_2\rangle_i - 2\langle\hat{p}_1\rangle_i\langle\hat{p}_3\rangle_i - 2\langle\hat{p}_2\rangle_i\langle\hat{p}_3\rangle_i) - \langle\hat{u}\rangle_\rho^2 - \langle\hat{v}\rangle_\rho^2 - \langle\hat{w}\rangle_\rho^2\end{aligned}$$

$$\begin{aligned}
 &= \sum_i P_i \frac{2}{3} \left(\langle (\Delta \hat{x}_1)^2 \rangle_i + \langle (\Delta \hat{x}_2)^2 \rangle_i + \langle (\Delta \hat{x}_3)^2 \rangle_i \right. \\
 &\quad \left. + \langle (\Delta \hat{p}_1)^2 \rangle_i + \langle (\Delta \hat{p}_2)^2 \rangle_i + \langle (\Delta \hat{p}_3)^2 \rangle_i \right) \\
 &\quad + \sum_i P_i \langle \hat{u} \rangle_i^2 - \left(\sum_i P_i \langle \hat{u} \rangle_i \right)^2 + \sum_i P_i \langle \hat{v} \rangle_i^2 - \left(\sum_i P_i \langle \hat{v} \rangle_i \right)^2 \\
 &\quad + \sum_i P_i \langle \hat{w} \rangle_i^2 - \left(\sum_i P_i \langle \hat{w} \rangle_i \right)^2, \tag{1.33}
 \end{aligned}$$

where $\langle \dots \rangle_i$ means the average in the product state $\hat{\rho}_{i1} \otimes \hat{\rho}_{i2} \otimes \hat{\rho}_{i3}$. Similar to the derivation in Ref. [26], we can apply the Cauchy-Schwarz inequality $\sum_i P_i \langle \hat{u} \rangle_i^2 \geq (\sum_i P_i \langle \hat{u} \rangle_i)^2$, and see that the last two lines in Eq. (1.33) are bounded below by zero. Also taking into account the sum uncertainty relation $\langle (\Delta \hat{x}_j)^2 \rangle_i + \langle (\Delta \hat{p}_j)^2 \rangle_i \geq |[\hat{x}_j, \hat{p}_j]| = 1/2$ ($j = 1, 2, 3$), we find that the total variance itself is bounded below by 1 (using $\sum_i P_i = 1$). Any total variance smaller than this boundary of 1 would imply that the quantum state concerned is not fully separable as in Eq. (1.32). But would this also imply that the quantum state is genuinely tripartite entangled in the sense that none of the parties can be separated from the others (as, for example, in the pure qubit states |GHZ) and |W)? This is obviously not the case and a total variance below 1 does not rule out the possibility of *partial separability*. The quantum state might still not be a genuine tripartite entangled state, since it might be written in one or more of the following forms⁴ [18]:

$$\hat{\rho} = \sum_i P_i \hat{\rho}_{i12} \otimes \hat{\rho}_{i3}, \quad \hat{\rho} = \sum_i P'_i \hat{\rho}_{i13} \otimes \hat{\rho}_{i2}, \quad \hat{\rho} = \sum_i P''_i \hat{\rho}_{i23} \otimes \hat{\rho}_{i1}. \tag{1.34}$$

Thus, in general, a violation of $\langle (\Delta \hat{u})^2 \rangle_\rho + \langle (\Delta \hat{v})^2 \rangle_\rho + \langle (\Delta \hat{w})^2 \rangle_\rho \geq 1$ does not necessarily witness genuine tripartite entanglement (a counterexample will be given below). However, it does witness genuine tripartite entanglement when the quantum state in question is pure and totally symmetric with respect to all three subsystems [28]. In that case, a possible separation of any individual subsystem,

$$\hat{\rho} = \hat{\rho}_{12} \otimes \hat{\rho}_3, \quad \hat{\rho} = \hat{\rho}_{13} \otimes \hat{\rho}_2, \quad \hat{\rho} = \hat{\rho}_{23} \otimes \hat{\rho}_1, \tag{1.35}$$

implies full separability, $\hat{\rho} = \hat{\rho}_1 \otimes \hat{\rho}_2 \otimes \hat{\rho}_3$. Hence a total variance below 1 negates the possibility of any form of separability in this case.

⁴A full classification of tripartite Gaussian states is given in Ref. [27] in analogy to that for qubits from Ref. [18]. In addition, necessary and sufficient three-mode inseparability criteria for Gaussian states are proposed in Ref. [27].

By extending the quadrature combinations in Eq. (1.31) from 3 to N parties (corresponding to the output modes of an inverse N -splitter) and performing a similar calculation as for $N = 3$ with an additional factor of $\sqrt{N-1}$ in the total momentum operator \hat{w} , we find that any N -mode state with modes $\hat{b}_1, \hat{b}_2, \dots, \hat{b}_N$ which is *fully separable*, $\hat{\rho} = \sum_i P_i \hat{\rho}_{i1} \otimes \hat{\rho}_{i2} \otimes \dots \otimes \hat{\rho}_{iN}$, obeys the inequality

$$\langle (\Delta \hat{p}'_1)^2 \rangle_\rho + \frac{\sum_{i=2}^N \langle (\Delta \hat{x}'_i)^2 \rangle_\rho}{N-1} \geq \frac{1}{2}. \quad (1.36)$$

Here, $\hat{p}'_1 \equiv \text{Im } \hat{b}'_1$, $\hat{x}'_2 \equiv \text{Re } \hat{b}'_2, \dots, \hat{x}'_N \equiv \text{Re } \hat{b}'_N$ are the corresponding output quadratures of the inverse N -splitter applied to the modes $\hat{b}_1, \hat{b}_2, \dots, \hat{b}_N$ [Eq. (1.28)]. Alternatively, one can also derive the following necessary condition for full separability [28],

$$\frac{\sum_{i,j}^N \langle (\Delta \hat{X}_{ij})^2 \rangle_\rho}{2(N-1)} + \langle (\Delta \hat{P})^2 \rangle_\rho \geq \frac{N}{2}. \quad (1.37)$$

In this inequality, $\hat{X}_{ij} = \hat{x}_i - \hat{x}_j$ and $\hat{P} = \sum_{i=1}^N \hat{p}_i$ are the relative positions and the total momentum of the relevant state with modes $\hat{b}_j = \hat{x}_j + i\hat{p}_j$.

The choice of the operators in the inequalities Eq. (1.36) and Eq. (1.37) relies upon the fact that the quantum fluctuations of these observables simultaneously vanish for maximum GHZ entanglement. This must be in agreement with their commutation relations, and indeed, we have

$$[\hat{X}_{ij}, \hat{P}] = [\hat{x}_i - \hat{x}_j, \hat{p}_i + \hat{p}_j] = 0, \quad (1.38)$$

for any N and i, j . Similarly, the output quadratures of the inverse N -splitter yield, for instance, for $N = 3$,

$$[\hat{p}_1 + \hat{p}_2 + \hat{p}_3, \hat{x}_2 - \hat{x}_3] = 0, \quad [\hat{p}_1 + \hat{p}_2 + \hat{p}_3, 2\hat{x}_1 - (\hat{x}_2 + \hat{x}_3)] = 0. \quad (1.39)$$

Both criteria in Eq. (1.36) and Eq. (1.37) represent necessary conditions for full separability, though they are not entirely equivalent [i.e., there are partially inseparable states that violate Eq. (1.37), but satisfy Eq. (1.36), see below]. Moreover, the criterion in Eq. (1.37) contains in some sense redundant observables. As we know from the previous section, N observables suffice to measure an N -party GHZ entangled state. These N observables are suitably chosen quadratures of the N output modes of an inverse N -splitter. Their detection simultaneously determines the total momentum and the $N-1$ relative positions $\hat{x}_1 - \hat{x}_2, \hat{x}_2 - \hat{x}_3, \dots$, and $\hat{x}_{N-1} - \hat{x}_N$ [Eq. (1.30)]⁵. However, in Eq. (1.37),

⁵The variances of the $N-1$ relative positions $\hat{x}_1 - \hat{x}_2, \hat{x}_2 - \hat{x}_3, \dots$, and $\hat{x}_{N-1} - \hat{x}_N$ are also available via the variances of the output quadratures of the inverse N -splitter. First, the variance of $\hat{x}'_N = \frac{1}{\sqrt{2}}(\hat{x}_{N-1} - \hat{x}_N)$

there are $1 + [N(N - 1)]/2$ different operators. Nevertheless, for two parties and modes, the conditions in Eq. (1.36) and Eq. (1.37) coincide and correspond to the necessary separability condition for arbitrary bipartite states given in Ref. [26].

In summary, we have shown in this section that the circuit for measuring GHZ entanglement also provides a sufficient inseparability criterion for arbitrary multi-party continuous-variable states (pure or mixed, Gaussian or non-Gaussian) of arbitrarily many parties. This criterion is experimentally accessible via linear optics and homodyne detections. The disadvantage of not being a necessary inseparability condition (not even for Gaussian states, see below) might be unsatisfactory from a theoretical point of view, but would not be an obstacle to experimental inseparability proofs. A more serious drawback, in particular when considering an experimental verification of multi-party entanglement, is the fact that without additional assumptions, for arbitrary states, the criteria presented in this section are in general not sufficient for genuine multi-party inseparability. They verify only partial inseparability. In the next section, we will give a simple example for this.

2.5 MULTI-PARTY ENTANGLED STATES

Partial multipartite entanglement. Let us investigate how the following pure three-mode state described by the Heisenberg operators

$$\begin{aligned} \hat{x}'_1 &= (e^{+r}\hat{x}_1^{(0)} + e^{-r}\hat{x}_2^{(0)})/\sqrt{2}, & \hat{p}'_1 &= (e^{-r}\hat{p}_1^{(0)} + e^{+r}\hat{p}_2^{(0)})/\sqrt{2}, \\ \hat{x}'_2 &= (e^{+r}\hat{x}_1^{(0)} - e^{-r}\hat{x}_2^{(0)})/\sqrt{2}, & \hat{p}'_2 &= (e^{-r}\hat{p}_1^{(0)} - e^{+r}\hat{p}_2^{(0)})/\sqrt{2}, \\ \hat{x}'_3 &= \hat{x}_3^{(0)}, & \hat{p}'_3 &= \hat{p}_3^{(0)}, \end{aligned} \quad (1.40)$$

behaves with respect to the multi-party inseparability criteria. Modes 1 and 2 are in a two-mode squeezed vacuum state [Eq. (1.18) and Eq. (1.20) for $N = 2$ and $r = r_1 = r_2$], and mode 3 is in the vacuum state. This three-party state is obviously only partially ⁶ entangled (it is an example for the second class of the five classes of three-mode Gaussian states in Ref. [27]). Applying an inverse “tritter” (three-splitter) to these modes, calculating the relevant output

corresponding to the last line in Eq. (1.30) is directly measurable. In addition, by converting the measured photocurrent into a light amplitude and “displacing” (feed-forward) \hat{x}'_{N-1} according to $\hat{x}'_{N-1} \rightarrow \hat{x}''_{N-1} = \hat{x}'_{N-1} - \frac{1}{\sqrt{3}}\hat{x}'_N = \sqrt{\frac{2}{3}}(\hat{x}_{N-2} - \hat{x}_{N-1})$, one can directly measure the variance of $\hat{x}_{N-2} - \hat{x}_{N-1}$ etc. Similarly, one would also employ this feed-forward technique in a multi-party quantum communication protocol that relies on the N classical results of an N -mode GHZ state measurement.

⁶note that we use the term “partially entangled” here for states which are not genuinely multi-party inseparable. In the literature, sometimes “partial entanglement” is also referred to as nonmaximum entanglement of two or more parties (in the sense that for two parties the Schmidt coefficients are not all equal). As discussed later, also the genuinely multi-party entangled continuous-variable states are only nonmaximally entangled due to the finite degree of the squeezing.

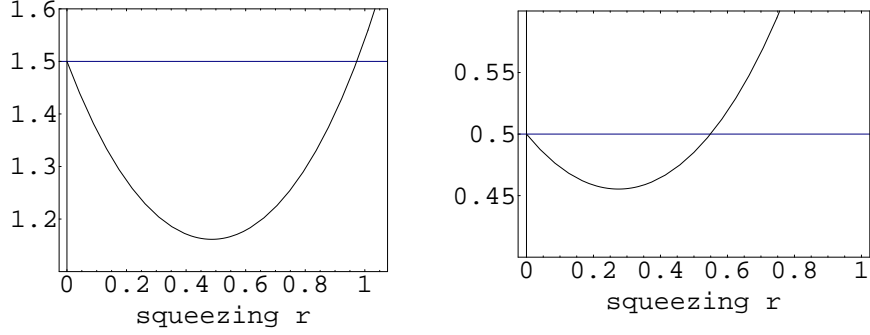


Figure 1.2 Application of the necessary conditions for full three-party separability. On the left: the inequality Eq. (1.42) with the boundary $3/2$ as a function of the squeezing r ; for $0 < r < 1$, the inequality is violated nearly everywhere. On the right: the inequality Eq. (1.41) with the boundary $1/2$ as a function of the squeezing r ; for $0 < r < 1$, the inequality is satisfied nearly as much as it is violated.

variances, and inserting them into Eq. (1.36) yields

$$\frac{1}{4} \left(\frac{1}{3} e^{+2r} + e^{-2r} \right) + \frac{1}{6} \geq \frac{1}{2}, \quad (1.41)$$

as a necessary condition for full separability. We find that equality holds for $r = 0$ which doesn't tell us anything, though we know, of course, that the state is fully separable in this case and must obey Eq. (1.36). For some finite squeezing r , the inequality Eq. (1.41) is illustrated in Fig. 1.2. Similarly, application of the criterion in Eq. (1.37) to the above state leads to

$$\frac{1}{4} (3e^{-2r} + \cosh 2r + 2) \geq \frac{3}{2}. \quad (1.42)$$

Again, equality holds for $r = 0$. In Fig. 1.2, also this condition is depicted for some finite squeezing r .

The comparison between the two conditions in this example demonstrates that they are not equivalent. For some squeezing, the partially entangled three-mode state violates Eq. (1.37) while satisfying Eq. (1.36). Moreover, both conditions can apparently be violated by an only partially entangled state. Hence, both their violation, though ruling out full separability, does not imply the presence of genuine multi-party entanglement. Another observation is that both conditions are satisfied for sufficiently large squeezing when the partial entanglement is sufficiently good. This confirms that the two conditions are necessary for full separability, but not sufficient, not even for a Gaussian state like that in our example. In fact, also the bipartite separability condition of Ref. [26] is both necessary and sufficient only for Gaussian states in a

certain standard form (where any Gaussian state can be transformed into this standard form via local operations). The partially entangled three-mode state here lacks the symmetry that is required for a state to violate the separability conditions whenever it contains some entanglement. We will now turn to a family of multipartite entangled states which are totally symmetric with respect to all their parties, which do always violate both conditions for full multi-party separability, and which are indeed genuinely multi-party entangled.

Genuine multipartite entanglement. Let us consider the output states of the entanglement-generating circuit in section 2.2. There, we applied an N -splitter to one momentum-squeezed (r_1) and $N - 1$ position-squeezed (r_2) vacuum modes to obtain the modes $\hat{a}'_1, \hat{a}'_2, \dots, \hat{a}'_N$ [Eq. (1.18)]. Now one can easily see that the first multi-party separability condition is violated for *any* nonzero squeezing $r_1 > 0$ or $r_2 > 0$, because application of an inverse N -splitter means

$$\begin{aligned} (\hat{a}''_1 \ \hat{a}''_2 \ \cdots \ \hat{a}''_N)^T &= \mathcal{U}^\dagger(N) (\hat{a}'_1 \ \hat{a}'_2 \ \cdots \ \hat{a}'_N)^T \\ &= \mathcal{U}^\dagger(N) \mathcal{U}(N) (\hat{a}_1 \ \hat{a}_2 \ \cdots \ \hat{a}_N)^T, \end{aligned} \quad (1.43)$$

with $\hat{a}_1, \hat{a}_2, \dots, \hat{a}_N$ from Eq. (1.19). Since $\mathcal{U}^\dagger(N) \mathcal{U}(N) = I$ (identity matrix), the squeezed quadratures of Eq. (1.20) can be directly inserted into Eq. (1.36) yielding a violation of $(e^{-2r_1} + e^{-2r_2})/4 \geq 1/2$ for any $r_1 > 0$ or $r_2 > 0$. Alternatively, using Eq. (1.21), the criterion in Eq. (1.37) becomes

$$\binom{N}{2} \frac{e^{-2r_2}}{2(N-1)} + \frac{N e^{-2r_1}}{4} = \frac{N}{4} (e^{-2r_1} + e^{-2r_2}) \geq \frac{N}{2}. \quad (1.44)$$

This condition is also violated for any $r_1 > 0$ or $r_2 > 0$. Due to their purity and total symmetry we conclude that the members of the family of states which emerge from the N -splitter circuit are genuinely multi-party entangled for any $r_1 > 0$ or $r_2 > 0$. This applies in particular to the case where $r_1 > 0$ and $r_2 = 0$, i.e., when only *one* squeezed light mode is required for the creation of genuine multipartite entanglement.

Independent of the inequalities Eq. (1.36) and Eq. (1.37), there are also other ways to see that these particular states are genuinely multi-party entangled. One simply has to find some form of entanglement in these states. For example, by tracing out modes 2 through N of the pure N -mode state given in Eq. (1.18), one finds that the remaining one-mode state is mixed, provided $r_1 > 0$ or $r_2 > 0$ [28]. Thus, the pure N -mode state is somehow entangled and hence genuinely multi-party entangled due to its complete symmetry. Note that in order to infer even only partial entanglement via tracing out parties, the N -mode state here has to be pure. In contrast, the multi-party inseparability criteria of section 2.4 may verify partial inseparability for any N -mode state.

From a conceptual point of view, it is very illuminating to analyze which states of the above family of N -mode states can be transformed into each other

via local squeezing operations [29]. For example, by applying local squeezers with squeezing s_1 and s_2 to the two modes of the bipartite state generated with only one squeezer [Eq. (1.20) for $N = 2$ with $r_2 = 0$], we obtain

$$\begin{aligned}
\hat{x}_1'' &= e^{-s_1} \hat{x}_1' = (e^{+r_1-s_1} \hat{x}_1^{(0)} + e^{-s_1} \hat{x}_2^{(0)})/\sqrt{2}, \\
\hat{p}_1'' &= e^{+s_1} \hat{p}_1' = (e^{+s_1-r_1} \hat{p}_1^{(0)} + e^{+s_1} \hat{p}_2^{(0)})/\sqrt{2}, \\
\hat{x}_2'' &= e^{-s_2} \hat{x}_2' = (e^{+r_1-s_2} \hat{x}_1^{(0)} - e^{-s_2} \hat{x}_2^{(0)})/\sqrt{2}, \\
\hat{p}_2'' &= e^{+s_2} \hat{p}_2' = (e^{+s_2-r_1} \hat{p}_1^{(0)} - e^{+s_2} \hat{p}_2^{(0)})/\sqrt{2}.
\end{aligned} \tag{1.45}$$

With the choice of $s_1 = s_2 = r_1/2 \equiv r$, the state in Eq. (1.45) is identical to a two-mode squeezed state built from two equally squeezed states [Eq. (1.20) for $N = 2$ with $r_1 \equiv r$, $r_2 \equiv r$]. The latter and the state produced with only one squeezer [Eq. (1.20) with $r_1 = 2r$ and $r_2 = 0$] are equivalent under local squeezing operations. This means that Alice and Bob sharing the state produced with one squeezer $r_1 = 2r$ have access to the same amount of entanglement as in the ‘‘canonical’’ two-mode squeezed state with squeezing $r = r_1/2$, $E_{\text{v.N.}} = [\cosh(r_1/2)]^2 \log[\cosh(r_1/2)]^2 - [\sinh(r_1/2)]^2 \log[\sinh(r_1/2)]^2$ [30]. For a given amount of entanglement, however, the canonical two-mode squeezed vacuum state has the least mean photon number. Conversely, for a given mean energy, the canonical two-mode squeezed vacuum state contains the maximum amount of entanglement possible.

Similar arguments apply to the states of more than two modes. From the family of N -mode states, the state with the least mean photon number is determined by the relation

$$e^{\pm 2r_1} = (N-1) \sinh 2r_2 \left[\sqrt{1 + \frac{1}{(N-1)^2 \sinh^2 2r_2}} \pm 1 \right]. \tag{1.46}$$

This relation is obtained by requiring each mode of the N -mode states to be symmetric or ‘‘unbiased’’ in the x and p variances [29]. Only for $N = 2$, we obtain $r_1 = r_2$. Otherwise, the first squeezer with r_1 and the $N - 1$ remaining squeezers with r_2 have different squeezing. In the limit of large squeezing, we may use $\sinh 2r_2 \approx e^{+2r_2}/2$ and approximate e^{+2r_1} of Eq. (1.46) by

$$e^{+2r_1} \approx (N-1)e^{+2r_2}. \tag{1.47}$$

We see that in order to produce the minimum-energy N -mode state, the single r_1 -squeezer is, in terms of the squeezing factor, $N - 1$ times as much squeezed as each r_2 -squeezer. However, also in this general N -mode case, the other N -mode states of the family can be converted into the minimum-energy states via local squeezing operations. This applies in particular to the N -mode states

produced with just a single squeezer and to those built from N equally squeezed states. As a result, due to the equivalence under local entanglement-preserving operations, with a single sufficiently squeezed state and beam splitters, arbitrarily many genuinely multi-party entangled modes can be created just as well as with N squeezers and beam splitters.

In contrast to the three-mode state given by Eq. (1.40), the output states of the N -splitter are totally symmetric under interchange of parties. This becomes more transparent when we look at the states in the Wigner representation. For simplicity, let us assume $r = r_1 = r_2$. The position-squeezed input states of the N -splitter circuit, for instance, have the Wigner function

$$W(x, p) = \frac{2}{\pi} \exp(-2e^{+2r}x^2 - 2e^{-2r}p^2). \quad (1.48)$$

Through the linear N -splitter operation, the total input Wigner function to the N -splitter (one momentum-squeezed and $N - 1$ position-squeezed vacuum modes),

$$\begin{aligned} W_{\text{in}}(\mathbf{x}, \mathbf{p}) &= \left(\frac{2}{\pi}\right)^N \exp(-2e^{-2r}x_1^2 - 2e^{+2r}p_1^2) \\ &\exp(-2e^{+2r}x_2^2 - 2e^{-2r}p_2^2) \exp(-2e^{+2r}x_3^2 - 2e^{-2r}p_3^2) \\ &\times \cdots \times \exp(-2e^{+2r}x_N^2 - 2e^{-2r}p_N^2), \end{aligned} \quad (1.49)$$

is transformed into the output Wigner function

$$\begin{aligned} W_{\text{out}}(\mathbf{x}, \mathbf{p}) &= \left(\frac{2}{\pi}\right)^N \exp \left\{ -e^{-2r} \left[\frac{2}{N} \left(\sum_{i=1}^N x_i \right)^2 + \frac{1}{N} \sum_{i,j}^N (p_i - p_j)^2 \right] \right. \\ &\quad \left. - e^{+2r} \left[\frac{2}{N} \left(\sum_{i=1}^N p_i \right)^2 + \frac{1}{N} \sum_{i,j}^N (x_i - x_j)^2 \right] \right\}. \end{aligned} \quad (1.50)$$

Here we have used $\mathbf{x} = (x_1, x_2, \dots, x_N)$ and $\mathbf{p} = (p_1, p_2, \dots, p_N)$. The pure-state Wigner function $W_{\text{out}}(\mathbf{x}, \mathbf{p})$ is always positive, *symmetric* among the N modes, and becomes peaked at $x_i - x_j = 0$ ($i, j = 1, 2, \dots, N$) and $p_1 + p_2 + \cdots + p_N = 0$ for large squeezing r . For $N = 2$, it exactly equals the well-known two-mode squeezed vacuum state Wigner function [13], which is proportional to $\delta(x_1 - x_2)\delta(p_1 + p_2)$ in the limit of infinite squeezing. As discussed previously, the state $W_{\text{out}}(\mathbf{x}, \mathbf{p})$ is genuinely N -partite entangled for any squeezing $r > 0$. The quantum nature of the cross correlations $x_i x_j$ and $p_i p_j$ appearing in $W_{\text{out}}(\mathbf{x}, \mathbf{p})$ for any $r > 0$ is also confirmed by the purity of

this state. This purity is guaranteed, since beam splitters turn pure states into pure states (it can also be checked via the correlation matrix of the Gaussian state $W_{\text{out}}(\mathbf{x}, \mathbf{p})$ [28]).

A nice example for a multi-party entangled state which is not a member of the above family of states and hence not totally symmetric with respect to all its modes is the $(M + 1)$ -mode state described by the Wigner function

$$\begin{aligned}
W_{\text{MQC}}(\mathbf{x}, \mathbf{p}) = & \left(\frac{2}{\pi}\right)^{M+1} \exp \left\{ -2e^{-2r_1} \left(\sin \theta_0 x_1 + \frac{\cos \theta_0}{\sqrt{M}} \sum_{i=2}^{M+1} x_i \right)^2 \right. \\
& -2e^{+2r_1} \left(\sin \theta_0 p_1 + \frac{\cos \theta_0}{\sqrt{M}} \sum_{i=2}^{M+1} p_i \right)^2 \\
& -2e^{+2r_2} \left(\cos \theta_0 x_1 - \frac{\sin \theta_0}{\sqrt{M}} \sum_{i=2}^{M+1} x_i \right)^2 \\
& -2e^{-2r_2} \left(\cos \theta_0 p_1 - \frac{\sin \theta_0}{\sqrt{M}} \sum_{i=2}^{M+1} p_i \right)^2 \\
& \left. - \frac{1}{M} \sum_{i,j=2}^{M+1} [(x_i - x_j)^2 + (p_i - p_j)^2] \right\}, \tag{1.51}
\end{aligned}$$

where $\mathbf{x} = (x_1, x_2, \dots, x_{M+1})$, $\mathbf{p} = (p_1, p_2, \dots, p_{M+1})$, and

$$\begin{aligned}
\frac{1}{\sqrt{M+1}} \leq \sin \theta_0 \leq \sqrt{\frac{M}{M+1}}, \tag{1.52} \\
e^{-2r_1} \equiv \frac{\sqrt{M} \sin \theta_0 - \cos \theta_0}{\sqrt{M} \sin \theta_0 + \cos \theta_0}, \quad e^{-2r_2} \equiv \frac{\sqrt{M} \cos \theta_0 - \sin \theta_0}{\sqrt{M} \cos \theta_0 + \sin \theta_0}.
\end{aligned}$$

The significance of this $(M + 1)$ -mode state is that it represents a kind of multiuser quantum channel (“MQC”) enabling optimal $1 \rightarrow M$ “telecloning” of arbitrary coherent states from one sender to M receivers [31]. Though not completely symmetric with respect to all $M + 1$ modes (but to modes 2 through $M + 1$), it is a pure Gaussian state which is indeed genuinely multi-party entangled. This can be seen, because none of the modes can be factored out of the total Wigner function. Despite its “asymmetry”, this state is not only partially multi-party entangled as is the asymmetric pure three-mode state given by Eq. (1.40). Of course, the bipartite entanglement between mode 1 on one side and modes 2 through $M + 1$ on the other side is the most important property of $W_{\text{MQC}}(\mathbf{x}, \mathbf{p})$ in order to be useful for $1 \rightarrow M$ telecloning [31].

The generation of the state $W_{\text{MQC}}(\mathbf{x}, \mathbf{p})$ is very similar to that of the above family of multi-party entangled states produced with an N -splitter: first make a bipartite entangled state by combining two squeezed vacua, one squeezed in p with r_1 and the other one squeezed in x with r_2 , at a phase-free beam splitter with reflectivity/transmittance parameter $\theta = \theta_0$. Then keep one half (the mode 1) and send the other half together with $M - 1$ vacuum modes through an M -splitter. The annihilation operators of the initial modes \hat{a}_j before the beam splitters, $j = 1, 2, \dots, M + 1$, are then given by

$$\begin{aligned}\hat{a}_1 &= \cosh r_1 \hat{a}_1^{(0)} + \sinh r_1 \hat{a}_1^{(0)\dagger}, \\ \hat{a}_2 &= \cosh r_2 \hat{a}_2^{(0)} - \sinh r_2 \hat{a}_2^{(0)\dagger}, \\ \hat{a}_i &= \hat{a}_i^{(0)},\end{aligned}\tag{1.53}$$

where $i = 3, 4, \dots, M + 1$.

By using the ideal phase-free beam splitter operation from Eq. (1.16), with $B_{kl}(\theta)$ this time representing an $(M + 1)$ -dimensional identity matrix with the entries I_{kk} , I_{kl} , I_{lk} , and I_{ll} replaced by the corresponding entries of the beam splitter matrix in Eq. (1.16), the MQC-generating circuit can be written as

$$\left(\hat{b}_1 \quad \hat{b}_2 \quad \cdots \quad \hat{b}_{M+1} \right)^T = \mathcal{U}_{\text{MQC}}(M + 1) \left(\hat{a}_1 \quad \hat{a}_2 \quad \cdots \quad \hat{a}_{M+1} \right)^T,\tag{1.54}$$

with

$$\begin{aligned}\mathcal{U}_{\text{MQC}}(M + 1) &\equiv B_{M M+1} \left(\sin^{-1} \frac{1}{\sqrt{2}} \right) B_{M-1 M} \left(\sin^{-1} \frac{1}{\sqrt{3}} \right) \\ &\quad \times \cdots \times B_{34} \left(\sin^{-1} \frac{1}{\sqrt{M-1}} \right) B_{23} \left(\sin^{-1} \frac{1}{\sqrt{M}} \right) \\ &\quad \times B_{12}(\theta_0).\end{aligned}\tag{1.55}$$

The first beam splitter, acting on modes \hat{a}_1 and \hat{a}_2 , has reflectivity/transmittance parameter $\theta \equiv \theta_0$. The remaining beam splitters represent an M -splitter. In Eq. (1.54), the output modes \hat{b}_j correspond to the $M + 1$ modes of the MQC state described by W_{MQC} in Eq. (1.51). Let us now return to the totally symmetric multipartite entangled states given by Eq. (1.18) and explore some of their properties. For simplicity, we will thereby focus on those states emerging from the N -splitter circuit which are created with input states equally squeezed in momentum and position, $r = r_1 = r_2$.

Nonlocality and other properties. In this paragraph, we will discuss some of the properties of the state $W_{\text{out}}(\mathbf{x}, \mathbf{p})$ in Eq. (1.50). This will further illustrate the character of $W_{\text{out}}(\mathbf{x}, \mathbf{p})$ as a nonmaximally entangled multi-party state.

One such property is that this state, despite having an always positive Wigner function, violates N -party Bell-type [2] (or Mermin-type [32]) inequalities imposed by local realism for any squeezing $r > 0$ [33]. The observables producing these violations are displaced photon-number parities rather than continuous variables such as x and p [34]. Like for the qubit states [32], the violations increase as the number of parties N grows. However, this increase becomes steadily smaller for larger N , as opposed to the exponential increase for the maximally entangled qubit GHZ states [32]. This discrepancy may be explained by the fact that the violations are exposed only for finite squeezing where the state $W_{\text{out}}(\mathbf{x}, \mathbf{p})$ is a *nonmaximally* entangled multi-party state [33]. Note that, in general, the violations of N -party inequalities imposed by local realism do not necessarily imply the presence of genuine multipartite entanglement. However, for the pure and symmetric states $W_{\text{out}}(\mathbf{x}, \mathbf{p})$, once again, proving some kind of entanglement means proving genuine multipartite entanglement.

In order to prove the nonlocality exhibited by the state $W(\mathbf{x}, \mathbf{p}) \equiv W_{\text{out}}(\mathbf{x}, \mathbf{p})$, let us now use the fact that the Wigner function is proportional to the quantum expectation value of a displaced parity operator [35, 34]:

$$W(\boldsymbol{\alpha}) = \left(\frac{2}{\pi}\right)^N \langle \hat{\Pi}(\boldsymbol{\alpha}) \rangle = \left(\frac{2}{\pi}\right)^N \Pi(\boldsymbol{\alpha}), \quad (1.56)$$

where $\boldsymbol{\alpha} = \mathbf{x} + i\mathbf{p} = (\alpha_1, \alpha_2, \dots, \alpha_N)$ and $\Pi(\boldsymbol{\alpha})$ is the quantum expectation value of the operator

$$\hat{\Pi}(\boldsymbol{\alpha}) = \bigotimes_{i=1}^N \hat{\Pi}_i(\alpha_i) = \bigotimes_{i=1}^N \hat{D}_i(\alpha_i) (-1)^{\hat{n}_i} \hat{D}_i^\dagger(\alpha_i). \quad (1.57)$$

The operator $\hat{D}_i(\alpha_i)$ is the displacement operator,

$$\hat{D}(\alpha) = \exp(\alpha \hat{a}^\dagger - \alpha^* \hat{a}), \quad (1.58)$$

acting on mode i . Thus, $\hat{\Pi}(\boldsymbol{\alpha})$ is a product of displaced parity operators given by

$$\hat{\Pi}_i(\alpha_i) = \hat{\Pi}_i^{(+)}(\alpha_i) - \hat{\Pi}_i^{(-)}(\alpha_i), \quad (1.59)$$

with the projection operators

$$\hat{\Pi}_i^{(+)}(\alpha_i) = \hat{D}_i(\alpha_i) \sum_{k=0}^{\infty} |2k\rangle \langle 2k| \hat{D}_i^\dagger(\alpha_i), \quad (1.60)$$

$$\hat{\Pi}_i^{(-)}(\alpha_i) = \hat{D}_i(\alpha_i) \sum_{k=0}^{\infty} |2k+1\rangle \langle 2k+1| \hat{D}_i^\dagger(\alpha_i), \quad (1.61)$$

corresponding to the measurement of an even (parity +1) or an odd (parity -1) number of photons in mode i . This means that each mode is now characterized by a dichotomic variable similar to the spin of a spin-1/2 particle or the single-photon polarization. Different spin or polarizer orientations from the original qubit based Bell inequality are replaced by different displacements in phase space. This set of two-valued measurements for each setting is just what we need for the nonlocality test.

In the case of N -particle systems, such a nonlocality test is possible using the N -particle generalization of the two-particle Bell-CHSH inequality [16]. This inequality is based on the following recursively defined linear combination of joint measurement results (in this paragraph, the symbol B does not refer to a beam splitter operation),

$$B_N \equiv \frac{1}{2}[\sigma(a_N) + \sigma(a'_N)]B_{N-1} + \frac{1}{2}[\sigma(a_N) - \sigma(a'_N)]B'_{N-1} = \pm 2, \quad (1.62)$$

where $\sigma(a_N) = \pm 1$ and $\sigma(a'_N) = \pm 1$ describe two possible outcomes for two possible measurement settings (denoted by a_N and a'_N) of measurements on the N th particle. Note, the expressions B'_N are equivalent to B_N but with all the a_i and a'_i swapped. Provided that $B_{N-1} = \pm 2$ and $B'_{N-1} = \pm 2$, Equation (1.62) is trivially true for a single run of measurements where $\sigma(a_N)$ is either +1 or -1 and similarly for $\sigma(a'_N)$. Induction proves Eq. (1.62) for any N when we take

$$B_2 \equiv [\sigma(a_1) + \sigma(a'_1)]\sigma(a_2) + [\sigma(a_1) - \sigma(a'_1)]\sigma(a'_2) = \pm 2. \quad (1.63)$$

Within the framework of local realistic theories with hidden variables $\boldsymbol{\lambda} = (\lambda_1, \lambda_2, \dots, \lambda_N)$ and the normalized probability distribution $P(\boldsymbol{\lambda})$, we obtain an inequality for the average value of $B_N \equiv B_N(\boldsymbol{\lambda})$,

$$\left| \int d\lambda_1 d\lambda_2 \dots d\lambda_N P(\boldsymbol{\lambda}) B_N(\boldsymbol{\lambda}) \right| \leq 2. \quad (1.64)$$

By the linearity of averaging, this is a sum of means of products of the $\sigma(a_i)$ and $\sigma(a'_i)$. For example, if $N = 2$, we obtain the CHSH inequality

$$|C(a_1, a_2) + C(a_1, a'_2) + C(a'_1, a_2) - C(a'_1, a'_2)| \leq 2, \quad (1.65)$$

with the correlation functions

$$C(a_1, a_2) = \int d\lambda_1 d\lambda_2 P(\lambda_1, \lambda_2) \sigma(a_1, \lambda_1) \sigma(a_2, \lambda_2). \quad (1.66)$$

Following Bell [2], an always positive Wigner function can serve as the hidden-variable probability distribution with respect to measurements corresponding to any linear combination of \hat{x} and \hat{p} . In this sense, the finitely squeezed two-mode squeezed state Wigner function could prevent the CHSH inequality from being violated when restricted to such measurements: $W(x_1, p_1, x_2, p_2) \equiv P(\lambda_1, \lambda_2)$. The same applies to the Wigner function in Eq. (1.50): $W(\mathbf{x}, \mathbf{p}) \equiv P(\boldsymbol{\lambda})$ could be used to construct correlation functions

$$C(\mathbf{a}) = \int d\lambda_1 d\lambda_2 \dots d\lambda_N P(\boldsymbol{\lambda}) \times \sigma(a_1, \lambda_1) \sigma(a_2, \lambda_2) \dots \sigma(a_N, \lambda_N), \quad (1.67)$$

where $\mathbf{a} = (a_1, a_2, \dots, a_N)$. However, for parity measurements on each mode with possible results ± 1 for each differing displacement, this would require unbounded δ -functions for the local objective quantities $\sigma(a_i, \lambda_i)$ [34], as in this case we have

$$C(\mathbf{a}) \equiv \Pi(\boldsymbol{\alpha}) = (\pi/2)^N W(\boldsymbol{\alpha}). \quad (1.68)$$

This relation directly relates the correlation function to the Wigner function and is indeed crucial for the nonlocality proof of the continuous-variable states in Eq. (1.50).

Let us begin by analyzing the nonlocal correlations exhibited by the entangled two-party state. For this state, the two-mode squeezed state in Eq. (1.50) with $N = 2$, we may investigate the combination [34]

$$\mathcal{B}_2 = \Pi(0, 0) + \Pi(0, \beta) + \Pi(\alpha, 0) - \Pi(\alpha, \beta), \quad (1.69)$$

which according to Eq. (1.65) satisfies $|\mathcal{B}_2| \leq 2$ for local realistic theories. Here, we have chosen the displacement settings $\alpha_1 = \alpha_2 = 0$ and $\alpha'_1 = \alpha$, $\alpha'_2 = \beta$.

Writing the states in Eq. (1.50) as

$$\Pi(\boldsymbol{\alpha}) = \exp \left\{ -2 \cosh 2r \sum_{i=1}^N |\alpha_i|^2 + \sinh 2r \left[\frac{2}{N} \sum_{i,j} (\alpha_i \alpha_j + \alpha_i^* \alpha_j^*) - \sum_{i=1}^N (\alpha_i^2 + \alpha_i^{*2}) \right] \right\}, \quad (1.70)$$

for $N = 2$ and $\alpha = \beta = i\sqrt{\mathcal{J}}$ with the real displacement parameter $\mathcal{J} \geq 0$ ⁷, we obtain $\mathcal{B}_2 = 1 + 2 \exp(-2\mathcal{J} \cosh 2r) - \exp(-4\mathcal{J} e^{+2r})$. In the limit of large

⁷This choice of two equal settings leads to the same result as that of Banaszek and Wodkiewicz [34] who used opposite signs: $\alpha = \sqrt{\mathcal{J}}$ and $\beta = -\sqrt{\mathcal{J}}$.

r (so $\cosh 2r \approx e^{+2r}/2$) and small \mathcal{J} , \mathcal{B}_2 is maximized for $\mathcal{J}e^{+2r} = (\ln 2)/3$, yielding $\mathcal{B}_2^{\max} \approx 2.19$ [34], which is a clear violation of the inequality $|\mathcal{B}_2| \leq 2$. Smaller violations also occur for smaller squeezing and larger \mathcal{J} . Indeed, for any nonzero squeezing, some violation takes place [33].

We will now consider more than two parties. Let us first examine the three-mode state by setting $N = 3$ in Eq. (1.50). According to the inequality of the correlation functions derived from Eq. (1.62)-(1.64), we have

$$|C(a_1, a_2, a'_3) + C(a_1, a'_2, a_3) + C(a'_1, a_2, a_3) - C(a'_1, a'_2, a'_3)| \leq 2. \quad (1.71)$$

Thus, for the combination

$$\mathcal{B}_3 = \Pi(0, 0, \gamma) + \Pi(0, \beta, 0) + \Pi(\alpha, 0, 0) - \Pi(\alpha, \beta, \gamma), \quad (1.72)$$

a contradiction to local realism is demonstrated by $|\mathcal{B}_3| > 2$. The corresponding settings here are $\alpha_1 = \alpha_2 = \alpha_3 = 0$ and $\alpha'_1 = \alpha$, $\alpha'_2 = \beta$, $\alpha'_3 = \gamma$. With the choice $\alpha = \sqrt{\mathcal{J}}e^{i\phi_1}$, $\beta = \sqrt{\mathcal{J}}e^{i\phi_2}$, and $\gamma = \sqrt{\mathcal{J}}e^{i\phi_3}$, we obtain

$$\begin{aligned} \mathcal{B}_3 &= \sum_{i=1}^3 \exp(-2\mathcal{J} \cosh 2r - \frac{2}{3}\mathcal{J} \sinh 2r \cos 2\phi_i) \\ &- \exp \left\{ -6\mathcal{J} \cosh 2r - \frac{1}{3}\mathcal{J} \sinh 2r \sum_{i \neq j}^3 [\cos 2\phi_i - 4 \cos(\phi_i + \phi_j)] \right\}. \end{aligned} \quad (1.73)$$

Apparently, because of the symmetry of the entangled three-mode state, equal phases ϕ_i should also be chosen in order to maximize \mathcal{B}_3 . The best choice is $\phi_1 = \phi_2 = \phi_3 = \pi/2$, which ensures that the positive terms in Eq. (1.73) become maximal and the contribution of the negative term minimal. Therefore, we again use equal settings $\alpha = \beta = \gamma = i\sqrt{\mathcal{J}}$ and obtain

$$\mathcal{B}_3 = 3 \exp(-2\mathcal{J} \cosh 2r + 2\mathcal{J} \sinh 2r/3) - \exp(-6\mathcal{J}e^{+2r}). \quad (1.74)$$

The violations of $|\mathcal{B}_3| \leq 2$ that occur with this result are similar to the violations of $|\mathcal{B}_2| \leq 2$ obtained for the two-mode state, but the $N = 3$ violations are even more significant than the $N = 2$ violations [33]. In the limit of large r (and small \mathcal{J}), we may use $\cosh 2r \approx \sinh 2r \approx e^{+2r}/2$ in Eq. (1.74). Then \mathcal{B}_3 is maximized for $\mathcal{J}e^{+2r} = 3(\ln 3)/16$: $\mathcal{B}_3^{\max} \approx 2.32$. This optimal choice requires smaller displacements \mathcal{J} than those of the $N = 2$ case for the same squeezing.

Let us now investigate the cases $N = 4$ and $N = 5$. From Eq. (1.62)-(1.64) with $N = 4$, the following inequality for the correlation functions can

be derived:

$$\begin{aligned}
& \frac{1}{2} |C(a_1, a_2, a_3, a'_4) + C(a_1, a_2, a'_3, a_4) + C(a_1, a'_2, a_3, a_4) \\
& + C(a'_1, a_2, a_3, a_4) + C(a_1, a_2, a'_3, a'_4) + C(a_1, a'_2, a_3, a'_4) \\
& + C(a'_1, a_2, a_3, a'_4) + C(a_1, a'_2, a'_3, a_4) + C(a'_1, a_2, a'_3, a_4) \\
& + C(a'_1, a'_2, a_3, a_4) - C(a'_1, a'_2, a'_3, a_4) - C(a'_1, a'_2, a_3, a'_4) \\
& - C(a'_1, a_2, a'_3, a'_4) - C(a_1, a'_2, a'_3, a'_4) - C(a_1, a_2, a_3, a_4) \\
& - C(a'_1, a'_2, a'_3, a'_4)| \leq 2 .
\end{aligned} \tag{1.75}$$

It is symmetric among all four parties as any inequality derived from Eq. (1.62)-(1.64) is symmetric among all parties. For the settings $\alpha_1 = \alpha_2 = \alpha_3 = \alpha_4 = 0$ and $\alpha'_1 = \alpha$, $\alpha'_2 = \beta$, $\alpha'_3 = \gamma$, $\alpha'_4 = \delta$, complying with local realism means $|\mathcal{B}_4| \leq 2$ where

$$\begin{aligned}
\mathcal{B}_4 = & \frac{1}{2} [\Pi(0, 0, 0, \delta) + \Pi(0, 0, \gamma, 0) + \Pi(0, \beta, 0, 0) \\
& + \Pi(\alpha, 0, 0, 0) + \Pi(0, 0, \gamma, \delta) + \Pi(0, \beta, 0, \delta) \\
& + \Pi(\alpha, 0, 0, \delta) + \Pi(0, \beta, \gamma, 0) + \Pi(\alpha, 0, \gamma, 0) \\
& + \Pi(\alpha, \beta, 0, 0) - \Pi(\alpha, \beta, \gamma, 0) - \Pi(\alpha, \beta, 0, \delta) \\
& - \Pi(\alpha, 0, \gamma, \delta) - \Pi(0, \beta, \gamma, \delta) - \Pi(0, 0, 0, 0) \\
& - \Pi(\alpha, \beta, \gamma, \delta)] .
\end{aligned} \tag{1.76}$$

Similarly, for $N = 5$ one finds

$$\begin{aligned}
\mathcal{B}_5 = & \frac{1}{2} [\Pi(0, 0, 0, \delta, \epsilon) + \Pi(0, 0, \gamma, 0, \epsilon) + \Pi(0, \beta, 0, 0, \epsilon) \\
& + \Pi(\alpha, 0, 0, 0, \epsilon) + \Pi(0, 0, \gamma, \delta, 0) + \Pi(0, \beta, 0, \delta, 0) \\
& + \Pi(\alpha, 0, 0, \delta, 0) + \Pi(0, \beta, \gamma, 0, 0) + \Pi(\alpha, 0, \gamma, 0, 0) \\
& + \Pi(\alpha, \beta, 0, 0, 0) - \Pi(\alpha, \beta, \gamma, \delta, 0) - \Pi(\alpha, \beta, \gamma, 0, \epsilon) \\
& - \Pi(\alpha, \beta, 0, \delta, \epsilon) - \Pi(\alpha, 0, \gamma, \delta, \epsilon) - \Pi(0, \beta, \gamma, \delta, \epsilon) \\
& - \Pi(0, 0, 0, 0, 0)] ,
\end{aligned} \tag{1.77}$$

which has to satisfy $|\mathcal{B}_5| \leq 2$ and contains the same settings as for $N = 4$, but in addition we have chosen $\alpha_5 = 0$ and $\alpha'_5 = \epsilon$.

We can now use the entangled states of Eq. (1.70) with $N = 4$ and $N = 5$ and apply the inequalities to them. For the same reason as for $N = 3$ (symmetry among all modes in the states and in the inequalities), the choice $\alpha = \beta = \gamma = \delta = \epsilon = i\sqrt{\mathcal{J}}$ appears to be optimal (maximizes positive terms and minimizes negative contributions).

With this choice, we obtain

$$\begin{aligned}
 \mathcal{B}_4 &= 2 \exp(-2\mathcal{J} \cosh 2r + \mathcal{J} \sinh 2r) \\
 &\quad - 2 \exp(-6\mathcal{J} \cosh 2r - 3\mathcal{J} \sinh 2r) \\
 &\quad + 3 \exp(-4\mathcal{J} \cosh 2r) - \frac{1}{2} \exp(-8\mathcal{J}e^{+2r}) - \frac{1}{2}, \\
 \mathcal{B}_5 &= 5 \exp(-4\mathcal{J} \cosh 2r + 4\mathcal{J} \sinh 2r/5) \\
 &\quad - \frac{5}{2} \exp(-8\mathcal{J} \cosh 2r - 24\mathcal{J} \sinh 2r/5) - \frac{1}{2}. \quad (1.78)
 \end{aligned}$$

Apparently, the maximum violation of $|\mathcal{B}_N| \leq 2$ (for our particular choice of settings) grows with increasing number of parties N [33]. The asymptotic analysis (large r and small \mathcal{J}) yields, for instance, for $N = 5$: $\mathcal{B}_5^{\max} \approx 2.48$ with $\mathcal{J}e^{+2r} = 5(\ln 2)/24$. For a given amount of squeezing, smaller displacements \mathcal{J} than those for $N \leq 4$ (at the same squeezing) are needed to approach this maximum violation. Another interesting observation is that in all four cases ($N = 2, 3, 4, 5$), violations occur for any nonzero squeezing [33]. This implies the presence of N -partite entanglement for any nonzero squeezing. Moreover, also for modest finite squeezing, the size of the violations (at optimal displacement \mathcal{J}) grows with increasing N [33].

Larger numbers of parties $N > 5$ were also considered in Ref. [33]. The degree of nonlocality of the continuous-variable states, if represented by the maximum violation of the corresponding Bell-type inequalities, seems to grow with an increasing number of parties. This growth, however, decelerates for larger numbers of parties. Thus, the ‘evolution’ of the continuous-variable states’ nonlocality with an increasing number of parties and the corresponding ‘evolution’ of nonlocality for the qubit GHZ states are qualitatively similar but quantitatively different with an exponential increase for the qubits. The reason for this may be that the qubit GHZ states are maximally entangled, whereas the continuous-variable states are nonmaximally entangled for any finite squeezing. Similarly, the N -party version of the nonmaximally entangled qubit state $|W\rangle$ yields a non-exponential increase of the maximum violations (by employing, for example, an analysis analogous to that here [36]). Note that the observation of the nonlocality of the continuous-variable states here requires small but nonzero displacements $\mathcal{J} \propto e^{-2r}$, which is not achievable when the singular maximally entangled states for infinite squeezing are considered.

Finally, the ‘unbiased’ minimum-energy states of the family of entangled N -mode states might yield larger violations. These states are not produced with N equal squeezers (as those states whose nonlocality we have analyzed here), but with one r_1 -squeezer and $N - 1$ r_2 -squeezers related as in Eq. (1.46). With growing N , the unbiased states increasingly differ from the states that we have used for the nonlocality test [see Eq. (1.47) for large squeezing]. On the other hand, the biased and the unbiased states are equivalent under local squeezing

operations and thus cannot differ in their potential nonlocality. In addition, this equivalence shows that also the unbiased states are only nonmaximally entangled for finite squeezing, which suggests that they also do not lead to an exponential increase of the violations as for the qubit GHZ states.

In section 2.1, we discussed some properties of pure, fully entangled states of three qubits. An important feature of these states is that a distinction can be made between two inequivalent classes: states from the first class can be converted into the state $|\text{GHZ}\rangle$ via SLOCC, but not into the state $|\text{W}\rangle$ (not even with arbitrarily small probability). For the second class, exactly the opposite holds. In several senses, the representative $|\text{GHZ}\rangle$ of the former class would be best described as a maximally entangled state, whereas the representative $|\text{W}\rangle$ of the latter class is nonmaximally entangled. A distinct feature of the maximum entanglement of $|\text{GHZ}\rangle$ is that after tracing out one qubit, the remaining qubit pair is in a separable mixed state⁸. Apparently, the entanglement of $|\text{GHZ}\rangle$ heavily relies on all three parties. By contrast, the entanglement of the state $|\text{W}\rangle$ is robust to some extent against disposal of one qubit. When tracing out one qubit of $|\text{W}\rangle$, the remaining pair shares a mixed entangled state. In the continuous-variable setting, we can make analogous observations. By interpreting the state $\int dx |x, x, x\rangle$ as the analogue of $|\text{GHZ}\rangle$, we see that

$$\text{Tr}_1 \int dx dx' |x, x, x\rangle \langle x', x', x'| = \int dx |x\rangle_{22} \langle x| \otimes |x\rangle_{33} \langle x|, \quad (1.79)$$

which is clearly a separable mixed state (and indeed not the maximally mixed state $\propto \int dx dx' |x, x'\rangle \langle x, x'|$). More interesting is the behaviour of a regularized version of $\int dx |x, x, x\rangle$. In order to apply bipartite inseparability criteria, let us trace out (integrate out) one mode of the Wigner function $W_{\text{out}}(\mathbf{x}, \mathbf{p})$ in Eq. (1.50) for $N = 3$,

$$\begin{aligned} \text{Tr}_1 W_{\text{out}}(\mathbf{x}, \mathbf{p}) &= \int dx_1 dp_1 W_{\text{out}}(\mathbf{x}, \mathbf{p}) \\ &\propto \exp \left[-2e^{+2r} \frac{e^{+2r} + 2e^{-2r}}{e^{-2r} + 2e^{+2r}} (x_2^2 + x_3^2) - 2e^{-2r} \frac{e^{-2r} + 2e^{+2r}}{e^{+2r} + 2e^{-2r}} (p_2^2 + p_3^2) \right. \\ &\quad \left. + 4e^{+2r} \frac{e^{+2r} - e^{-2r}}{e^{-2r} + 2e^{+2r}} x_2 x_3 + 4e^{-2r} \frac{e^{-2r} - e^{+2r}}{e^{+2r} + 2e^{-2r}} p_2 p_3 \right]. \end{aligned} \quad (1.80)$$

⁸However, remember that this is not the maximally mixed state for two qubits. Only when tracing out two parties do we end up having the maximally mixed one-qubit state.

From the resulting Gaussian two-mode Wigner function, we can extract the inverse correlation matrix. For Gaussian N -mode states with zero mean values, the Wigner function is given by

$$W(\boldsymbol{\xi}) = \frac{1}{(2\pi)^N \sqrt{\det \mathbf{V}}} \exp \left\{ -\frac{1}{2} \boldsymbol{\xi} \mathbf{V}^{-1} \boldsymbol{\xi}^T \right\}, \quad (1.81)$$

with the $2N$ -dimensional vector $\boldsymbol{\xi}$ having the quadrature pairs of all N modes as its components,

$$\boldsymbol{\xi} = (x_1, p_1, x_2, p_2, \dots, x_N, p_N), \quad \hat{\boldsymbol{\xi}} = (\hat{x}_1, \hat{p}_1, \hat{x}_2, \hat{p}_2, \dots, \hat{x}_N, \hat{p}_N), \quad (1.82)$$

and with the $2N \times 2N$ correlation matrix \mathbf{V} having as its elements the second moments (symmetrized according to the Weyl correspondence),

$$\begin{aligned} \text{Tr}[\hat{\rho}(\Delta\hat{\xi}_i\Delta\hat{\xi}_j + \Delta\hat{\xi}_j\Delta\hat{\xi}_i)/2] &= \langle (\hat{\xi}_i\hat{\xi}_j + \hat{\xi}_j\hat{\xi}_i)/2 \rangle \\ &= \int W(\boldsymbol{\xi}) \xi_i \xi_j d^{2N} \xi = V_{ij}, \end{aligned} \quad (1.83)$$

where $\Delta\hat{\xi}_i = \hat{\xi}_i - \langle \hat{\xi}_i \rangle = \hat{\xi}_i$ for zero mean values. The last equality defines the correlation matrix for any quantum state, but for Gaussian states of the form Eq. (1.81), the Wigner function is completely determined by the second-moment correlation matrix. Now we can calculate the bipartite correlation matrix of the state in Eq. (1.80),

$$\mathbf{V} = \frac{1}{12} \begin{pmatrix} e^{+2r} + 2e^{-2r} & 0 & 2 \sinh 2r & 0 \\ 0 & e^{-2r} + 2e^{+2r} & 0 & -2 \sinh 2r \\ 2 \sinh 2r & 0 & e^{+2r} + 2e^{-2r} & 0 \\ 0 & -2 \sinh 2r & 0 & e^{-2r} + 2e^{+2r} \end{pmatrix}. \quad (1.84)$$

We could have also obtained this two-mode correlation matrix by extracting the three-mode correlation matrix \mathbf{V} of the state $W_{\text{out}}(\mathbf{x}, \mathbf{p})$ in Eq. (1.50) with $N = 3$ and ignoring all entries involving mode 1 [or equivalently by explicitly calculating the correlations between modes 2 and 3 with the Heisenberg operators in Eq. (1.18) for $r = r_1 = r_2$ and $N = 3$]. The resulting two-mode state is a (mixed) inseparable state for any nonzero squeezing $r > 0$. Note that, for instance, the total variance in Eq. (1.37) with $N = 2$ becomes for this state $(5e^{-2r} + e^{+2r})/6$, which drops below the boundary of 1 only for sufficiently small nonzero squeezing, but approaches infinity as the squeezing increases. However, we can easily verify the state's inseparability for any $r > 0$ by looking at the necessary two-party separability condition in product form given in Ref. [37]. We find that

$$\langle [\Delta(\hat{x}_2 - \hat{x}_3)]^2 \rangle \langle [\Delta(\hat{p}_2 + \hat{p}_3)]^2 \rangle = (2e^{-4r} + 1)/12, \quad (1.85)$$

which drops below the separability boundary of $1/4$ for any $r > 0$. Of course, also the necessary and sufficient partial transpose criterion from Ref. [14] indicates entanglement for any $r > 0$ [28]. Recall that by first taking the “infinite-squeezing limit” and then tracing out one mode, we had obtained a separable state [Eq. (1.79)]. That was what we expected according to the result for the maximally entangled qubit state $|\text{GHZ}\rangle$.

So after all, we confirm what we had intuitively expected: the tripartite state $W_{\text{out}}(\mathbf{x}, \mathbf{p})$ for finite squeezing is a nonmaximally entangled state like the qubit state $|\text{W}\rangle$. Only for infinite squeezing does it approach the maximally entangled state $\int dx |x, x, x\rangle$, the analogue of $|\text{GHZ}\rangle$. This result reflects what is known for two parties. The two-mode squeezed state $W_{\text{out}}(\mathbf{x}, \mathbf{p})$ with $N = 2$ becomes a maximally entangled state $\int dx |x, x\rangle$, such as the Bell state $(|00\rangle + |11\rangle)/\sqrt{2}$, only for infinite squeezing. For finite squeezing, it is known to be nonmaximally entangled.

3. CONCLUSIONS

Let us conclude by asking whether we were able to find answers to the questions posed at the beginning of this chapter: how can we generate, measure, and (theoretically and experimentally) verify genuine multipartite entangled states for continuous variables? How do the continuous-variable states compare to their qubit counterparts with respect to various properties?

As for the generation, we demonstrated that genuinely N -party entangled states are producible with squeezed light resources and beam splitters. In particular, one sufficiently squeezed light mode is in principle the only resource needed to create any degree of genuine multi-party entanglement by means of linear optics. The resulting states, though genuinely multi-party entangled, are always nonmaximally entangled multi-party states due to the finite amount of the squeezing. They behave like the N -party versions of the qubit state $|\text{W}\rangle$. First, they also contain bipartite entanglement readily available between any pair of modes (just as $|\text{W}\rangle$ and as opposed to the qubit state $|\text{GHZ}\rangle$). Secondly, they yield a non-exponential increase of violations of multi-party Bell-type inequalities for growing number of parties (as for $|\text{W}\rangle$ and different from the qubit state $|\text{GHZ}\rangle$ for which the increase is exponential).

Furthermore, we have seen that by inverting the circuits for generating genuine but nonmaximum multi-party entanglement, one can perform projection measurements onto the maximally entangled multi-party (GHZ) basis for continuous variables. In contrast to the difficulties in performing such measurements for photonic qubits within the framework of linear optics, continuous-variable GHZ measurements only require beam splitters and homodyne detectors. In addition, we showed that the circuits for measuring maximum GHZ entanglement are also applicable to the theoretical and experimental verifica-

tion of the nonmaximum entanglement of the multi-party states (which are those producible in the laboratory). The circuits provide a necessary condition for full separability of any N -partite N -mode state (pure or mixed, Gaussian or non-Gaussian) with any number of modes N . However, this condition is not sufficient for full separability and, more importantly, its violation does not verify genuine but only partial multipartite entanglement. For the theoretical verification of genuine multipartite entanglement, additional assumptions have to be taken into account such as the total symmetry of the relevant states. Therefore, an unambiguous experimental proof of genuine multipartite entanglement of continuous-variable states was not proposed in this chapter. A possible approach to this would be to consider the violation of stricter N -party Bell-type inequalities which cannot be violated by only partially entangled states. However, the experimental nonlocality test would then rely on observables such as the photon number parity, and hence become unfeasible with current technology. More desirable would be a test for genuine multipartite entanglement that is solely based on linear optics and efficient homodyne detections.

Acknowledgements. This work was partly supported by QUICOV under the IST-FET-QJPC programme, by a DAAD Doktorandenstipendium, and by the DFG (Deutsche Forschungsgemeinschaft).

References

- [1] E. Schmidt, *Math. Annalen* **63**, 433 (1906).
- [2] J. S. Bell, *Physics (N.Y.)* **1**, 195 (1964).
- [3] C. H. Bennett *et al.*, *Phys. Rev. A* **53**, 2046 (1996).
- [4] C. H. Bennett *et al.*, *Phys. Rev. A* **54**, 3824 (1996).
- [5] R. F. Werner, *Phys. Rev. A* **40**, 4277 (1989).
- [6] A. Peres, *Phys. Rev. Lett.* **77**, 1413 (1996).
- [7] M. Horodecki, P. Horodecki, and R. Horodecki, *Phys. Lett. A* **223**, 1 (1996).
- [8] M. Horodecki, P. Horodecki, and R. Horodecki, *Phys. Rev. Lett.* **80**, 5239 (1998).
- [9] D. P. DiVincenzo *et al.*, *Phys. Rev. A* **61**, 062312 (2000).
- [10] M. Horodecki and P. Horodecki, *Phys. Rev. A* **59**, 4206 (1999).
- [11] R. Horodecki, P. Horodecki, and M. Horodecki, *Phys. Lett. A* **210**, 377 (1996).
- [12] M. A. Nielsen and J. Kempe, *Phys. Rev. Lett.* **86**, 5184 (2001).
- [13] D. F. Walls and G. J. Milburn, *Quantum Optics*, Springer Verlag Berlin Heidelberg New York (1994).
- [14] R. Simon, *Phys. Rev. Lett.* **84**, 2726 (2000).

- [15] D. M. Greenberger, M. A. Horne, A. Shimony, and A. Zeilinger, *Am. J. Phys.* **58**, 1131 (1990).
- [16] D. N. Klyshko, *Phys. Lett. A* **172**, 399 (1993); N. Gisin and H. Bechmann-Pasquinucci, *Phys. Lett. A* **246**, 1 (1998).
- [17] W. Dür, G. Vidal, and J. I. Cirac, *Phys. Rev. A* **62**, 062314 (2000).
- [18] W. Dür, J. I. Cirac, and R. Tarrach, *Phys. Rev. Lett.* **83**, 3562 (1999).
- [19] P. van Loock and S. L. Braunstein, *Phys. Rev. Lett.* **84**, 3482 (2000).
- [20] M. Dušek, Los Alamos arXive quant-ph/0107119 (2001).
- [21] E. Knill, R. Laflamme, and G. J. Milburn, *Nature* **409**, 46 (2001).
- [22] A. Furusawa *et al.*, *Science* **282**, 706 (1998).
- [23] D. Bouwmeester *et al.*, *Phys. Rev. Lett.* **82**, 1345 (1999).
- [24] D. Boschi *et al.*, *Phys. Rev. Lett.* **80**, 1121 (1998).
- [25] S. Bose, V. Vedral, and P. L. Knight, *Phys. Rev. A* **57**, 822 (1998).
- [26] L.-M. Duan *et al.*, *Phys. Rev. Lett.* **84**, 2722 (2000).
- [27] G. Giedke *et al.*, *Phys. Rev. A* **64**, 052303 (2001).
- [28] P. van Loock, *Fortschr. d. Phys.*, to appear.
- [29] W. P. Bowen, P. K. Lam, and T. C. Ralph, Los Alamos arXive quant-ph/0104108 (2001).
- [30] S. J. van Enk, *Phys. Rev. A* **60**, 5059 (1999).
- [31] P. van Loock and S. L. Braunstein, *Phys. Rev. Lett.* **87**, 247901 (2001).
- [32] N. D. Mermin, *Phys. Rev. Lett.* **65**, 1838 (1990).
- [33] P. van Loock and S. L. Braunstein, *Phys. Rev. A* **63**, 022106 (2001).
- [34] K. Banaszek and K. Wodkiewicz, *Phys. Rev. A* **58**, 4345 (1998).
- [35] A. Royer, *Phys. Rev. A* **15**, 449 (1977); H. Moya-Cessa and P. L. Knight, *Phys. Rev. A* **48**, 2479 (1993).
- [36] G. Li *et al.*, *J. of Mod. Opt.* **49**, 237 (2002).
- [37] S. M. Tan, *Phys. Rev. A* **60**, 2752 (1999).